Available online at www.sciencedirect.com
SCIENCE DIRECT
Nuclear Instruments and Methods in Physics Research A 513 (2003) 143–146
NUCLEAR INSTRUMENTS & METHODS IN PHYSICS RESEARCH Section A
www.elsevier.com/locate/nima

Development of arrays of transition edge sensors for application in X-ray astronomy

Marcel P. Bruijn[a,*], Wouter M. Bergmann Tiest[a], Henk F.C. Hoevers[a], Eric Krouwer[a], Jan van der Kuur[a], Marcel L. Ridder[a], Zakaria Moktadir[b], Remco Wiegerink[b], Dick van Gelder[b], Miko Elwenspoek[b]

[a] *SRON National Institute for Space Research, Sorbonnelaan 2, 3584 CA Utrecht, The Netherlands*
[b] *MESA+ research institute, University of Twente, P.O. Box 217, 7500 AE Enschede, The Netherlands*

Abstract

The development of an array of voltage biased superconducting transition edge microcalorimeters is described. This work is directed to an application in future X-ray Astronomy missions, such as Constellation-X (USA) and the X-ray Evolving Universe Spectroscopy Mission (XEUS, Europe). After several years of very successful development of single pixel microcalorimeters (SRON showed a record energy resolution $\Delta E_{\mathrm{FWHM}} = 3.9\,\mathrm{eV}$ for 5.9 keV photons, combined with an effective time constant of 150 μs and high X-ray absorption efficiency (94%)) work towards an array of 32×32 pixels has started. Aiming at a prototype of 5×5 pixels, several options for fabrication, using micromachining techniques are under study, both experimentally and theoretically. Measurement of thermal transport in detector support structures at sub-Kelvin temperatures indicates ballistic phonon transport. The detector development is accompanied by finite element modeling.

PACS: 07.07.Df; 44.10.+I; 66.70.+f; 85.25.Oj; 85.85.+j; 95.55.Ka

Keywords: Microcalorimeter; X-ray astronomy; Imaging array; X-ray detector; Cryogenic sensor; Micro machining; XEUS

1. Introduction

In the understanding of the evolution of the very early universe, X-ray astronomy plays a key role. It enables the study of hot baryonic matter, in particular the intra cluster medium, the true intergalactic medium, and massive black holes. Future space astronomy missions like XEUS are presently being defined and are based on high resolution X-ray spectroscopy with significantly improved sensitivity and imaging capabilities, compared to the present X-ray observatories. Key elements are huge X-ray mirrors and detectors with challenging specifications. The detectors for the energy range 0.1 to 10 keV should combine high resolution ($\Delta E_{\mathrm{FWHM}} < 5\,\mathrm{eV}$ for 5.9 keV photons and 2 eV for 1 keV photons), a time constant smaller than 100 μs, and high efficiency (>90% up to 7 keV) with imaging capabilities of typically 32×32 pixels [1]. The type of detector,

*Corresponding author.:Tel.: +31-30-253-5600; fax: +31-30-254-0860.
E-mail address: m.p.bruijn@sron.nl (M.P. Bruijn).

0168-9002/$ - see front matter © 2003 Elsevier B.V. All rights reserved.
doi:10.1016/j.nima.2003.08.019

which is considered as most promising, is an array of voltage biased superconducting transition edge microcalorimeters [2], operated at sub-Kelvin temperatures. In Section 2 we will address briefly the status of development of single pixel microcalorimeters. Section 3 will indicate the critical development areas for array structures, followed by a description of the processing routes under investigation in Section 4. Preliminary results from a study of thermal transport properties, essential for the operation and design, are presented in Section 5.

2. Single pixel microcalorimeters

The basic physics and theoretical performance of a voltage-biased detector with a superconductor-to-normal phase transition thermometer (TES) are well established [2,3] and will not be repeated here. Some useful expressions are:

$\Delta E_{\mathrm{FWHM}} = 2.36\ \xi\ (k_{\mathrm{B}}\ T^2\ C)^{\frac{1}{2}}$, with k_{B} Bolzmann's constant, T the operating temperature and C the heat capacity of absorber and thermometer. ξ is a factor depending on the steepness of the superconducting transition (resistance $R(T)$) of the TES, represented by $\alpha = \mathrm{d}(\log R)/\mathrm{d}(\log T)$, and the exponent n of the power law that governs the heat link (the power flow is proportional to $T^n - T^n_{\mathrm{bath}}$). ξ is set point dependent and its typical value is about unity for representative microcalorimeters.

The effective time constant $\tau_{\mathrm{e}} = (C/G)/(1+\alpha/n)$, where G is the thermal conductance to the bath. The effective time constant is shorter than the intrinsic time constant C/G due to electrothermal feedback in the sensor.

The best present sensors, as produced and measured at SRON have an energy resolution $\Delta E_{\mathrm{FWHM}} = 3.9\,\mathrm{eV}$ for 5.9 keV photons, combined with an effective time constant of 150 μs and 90% X-ray absorption efficiency [4]. This level of performance, very close to the theoretical limit, is amongst the best-reported values in literature [5, 6]. The experience with single pixel sensors, produced on large (4 mm square), closed silicon nitride membranes, forms the basis for the design of the array structures.

3. Microcalorimeter arrays

An imaging microcalorimeter could be constructed using two principles:

1. Intrinsic 1D or 2D sensors, based on thermal diffusion in a large absorber and using 2 or 4 thermometers.
2. Pixel arrays.

Comparing the first scheme to the second, the energy resolution is degraded because of the larger heat capacity and the achievable count rate will be considerably lower due to pile up of pulses. For the XEUS application a pixel array is a far better option, even when the increased readout complexity is taken into account.

The critical development areas of arrays have their origin in the following design constraints:

1. Each pixel should have the same thermal link to the heat bath.
2. Given the tight efficiency demands, the filling factor must be >90%, so the pixels must be close packed.
3. The electrical and thermal cross talk between the pixels must be small enough not to degrade the energy resolution.
4. Fabrication feasibility and ruggedness.

Constraint 1 sets serious limits to the lateral thermal gradients that are allowed. Because of insufficient knowledge and data in the literature of the relevant thermal transport properties of materials and interfaces at these low operating temperatures, some lithographic tunability must be built in. Characterization of thermal properties is an important development area; a first result is described in Section 5.

Constraint 2 limits the available space for thermal connections and, more important, for electrical wiring. Options under investigation to relieve the dense wiring structures are (a) splitting the array vertically in more layers, or (b) by conducting the wiring vertically through the wafer to a fan out wafer. It also requires the need for a "mushroom shaped" absorber, as schematically depicted in Figs. 2 and 3. These structures have been reported in [7] and SRON also showed promising single pixel response ($\Delta E_{FWHM} = 5$ eV @ 5.9 keV) with such types of absorber [8].

Constraints 3 and 4 have not been studied experimentally so far. Instead we have started finite element modeling (FEM) of cross talk. This will also cause a drive for further development of the pulse processing algorithms. Moreover, the mechanical strength of etched nitride membranes was modeled using FEM, resulting in design guidelines. Experi-mental verification of these results is planned soon.

Two other important areas of development for the cryogenic sensor array are defined and under study:

- The read-out of the array is far from trivial. SQUID (Superconducting Quantum Interference Device) based pre-amplifiers must be specifically optimized for this application. For readout of large arrays, Time Domain Multiplexing [9] and Frequency Domain Multiplexing [10] are considered.
- For cooling of the sensor array a compact, rechargable and space qualified ADR (Adiabatic Demagnetization Refrigerator) is under development.

4. Design and processing routes

For the 5×5 prototype sensor array two different processing routes will be pursued. The design of the thermometer, absorber and nitride cooling link is in principle identical for both routes, see Fig. 1. The thermometer, a Ti/Au bilayer, has a critical temperature between 80 and 100 mK. The Bi absorber, with thin Cu thermalization layer, is 7 μm thick.

The difference is the formation of the supporting structure. In route 1 this structure is formed by etching deep, vertical slots in the backside of a Si [110] wafer, using anisotropic wet etching, see Fig. 2. The resulting walls have a {111} orientation and a smooth surface.

In route 2 we create a shallow cavity underneath the membrane by surface micromachining techniques, using a poly Si sacrificial layer, see Fig. 3. The cavity is opened at the end of the process, by wet TMAH etching from the front side or from the backside through a dry etched access hole. The advantage of route 2 is a better thermal ground for the pixel.

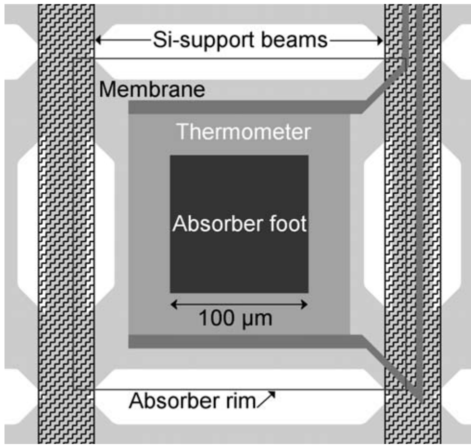

Fig. 1. Basic layout of a sensor pixel (top view). The thermal conductance to the cold bath can be tuned by etching slots in a nitride membrane. The Si support beams under the membrane are either left after backside wet etching into a wafer, or thin deposited poly Si ridges. For clarity only the two wiring lines to this pixel are drawn. Wiring from other pixels also runs across the beams.

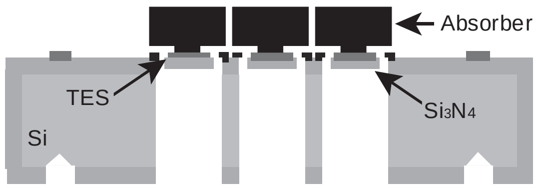

Fig. 2. Schematic side view of a pixel array, formed by route 1. Slots are wet etched into a Si_3N_4 coated Si[110] wafer. The pixel structure on the top is formed by e-beam evaporation, sputter deposition, etching and lift-off processing techniques. The Cu/Bi absorbers have a "mushroom" shape for close packing.

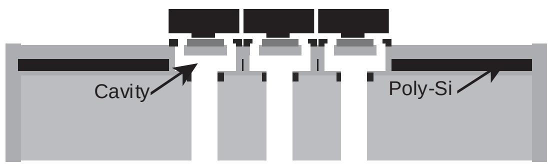

Fig. 3. Schematic side view of a pixel array, formed by route 2. A poly-Si sacrificial layer is used to create a cavity under each pixel. Access to the cavity is either from top or bottom side.

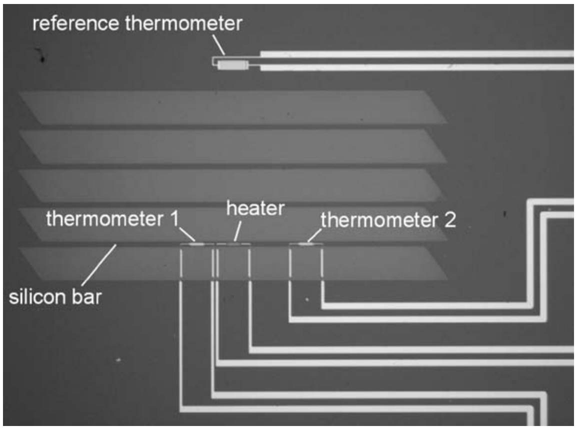

Fig. 4. Photograph of an experimental device. On one of the 40 μm wide etched Si-bars, a Cu heater and two Ti/Au bi-layer thermometers were lithographed. After cool down to a base temperature of 20 mK, the power through the heater is varied and the thermometers are heated to the normal state.

5. Thermal transport at low temperatures

Refering to constraint 1 in Section 3, a good thermal transport in the support structure is very important. At sub-Kelvin temperatures, in dielectric solids, the heat conduction by phonons can become dominated by scattering from surfaces, when the mean free path for scattering at bulk impurities and defects becomes comparable or larger than sample dimensions. Depending on the roughness of the surfaces, phonons scatter diffusively or speculary. The latter mode, also called ballistic transport, is prefered.

The thermal conductivity of Si-beams, fabricated using route 1, was measured, using a setup as presented in Fig. 4. The results were analized by comparing the experimental temperatures to a modeled profile. We have proposed a description, using the mean free path, to treat surface scattering by finite element modeling of heat flow in micromachined structures [11]. The phonon mean free path obtained from these data ($150 \pm 50\,\mu m$), indicates a cross-over from diffuse to specular phonon reflection. These preliminary results enable us to model the thermal performance of our array sensors. More accurate thermal measurements are planned for the near future.

6. Concluding remarks

In this paper, we have presented our development activities of microcalorimeter arrays for application in X-ray spectroscopy. First experimental results of thermal conductivity measurements feed the modeling of array performance.

Acknowledgements

Part of this work is supported by a research grant from the Nederlandse Organisatie voor Wetenschappelijk Onderzoek (NWO), and by a contract of the ESA technological research programme for the development of an imaging microcalorimeter array for XEUS.

References

[1] P.A.J. de Korte, et al., SPIE Proc. 3766 (1999) 103.
[2] K.D. Irwin, Appl. Phys. Lett. 66 (1995) 1998.
[3] K.D. Irwin, G.C. Hilton, D.A. Wollman, J.M. Martinis, J. Appl. Phys. 83 (1998) 3978.
[4] W.M. Bergmann Tiest, H.F.C Hoevers, M.P. Bruijn, W.A. Mels, M.L. Ridder, P.A.J. de Korte, M.E. Huber, AIP Conf. Proc. 605 (2002) 199.
[5] K.D. Irwin, G.C. Hilton, J.M. Martinis, S. Deiker, N. Bergren, S.W. Nam, D.A. Rudman, D.A. Wollman, Nucl. Instr. and Meth. A 444 (2000) 184.
[6] C.K. Stahle, P. Brekosky, E. Figueroa-Feliciano, F.M. Finkbeiner, J.D. Gygax, M.J. Li, M.A. Lindeman, F. Scott Porter, N. Tralshawala, SPIE Proc. 4140 (2000) 367.
[7] N. Tralshawala, et al., Nucl. Instr. and Meth. A 444 (2000) 188.
[8] W.M. Bergmann Tiest et al., NIST Workshop on Noise in TES microcalorimeters, April 25, 2002, unpublished.
[9] K.D. Irwin, Physica C 368 (2002) 203.
[10] M. Kiviranta, H. Seppä, J. van der Kuur, P. de Korte, Proceedings of Far IR, sub-mm and mm Detector Technology Workshop, Monterey 1 – 3 April 2002, to be published.
[11] Z. Moktadir, M.P. Bruijn, R. Wiegerink, M. Elwenspoek, M. Ridder, W.A. Mels, Proceedings of IEEE Sensors 2002, Paper 37.3, Orlando, 11 –14 June, 2002.